

DETECTION OF KETENIMINE (CH₂CNH) IN SAGITTARIUS B2(N) HOT CORES

F. J. LOVAS,¹ J. M. HOLLIS,² ANTHONY J. REMIJAN,³ AND P. R. JEWELL³

Received 2006 April 19; accepted 2006 May 31; published 2006 June 28

ABSTRACT

Ketenimine (CH₂CNH) has been detected in absorption toward the star-forming region Sagittarius B2(N) with the 100 m Green Bank Telescope by means of three rotational transitions: 7₁₆–8₀₈ at 41.5 GHz, 8₁₉–9₀₉ at 23.2 GHz, and 9₁₈–10₁₀ at 4.9 GHz. Ketenimine has a sparse rotational spectrum below 50 GHz. From transition line strength arguments, the spectral lines found are the ones most likely to be detected, and they occur in spectral regions that have little possibility of confusion with other molecular species. Partially resolved hyperfine structure is apparent in the 4.9 GHz transition, which has energy levels ~50 K above the ground-state level; the absorption seen in this transition appears to be emanating from gas in close proximity to the LMH hot core that has a systemic LSR velocity of +64 km s⁻¹. By comparison, the 41.5 and 23.2 GHz transitions have lower energy levels of ~33 and ~41 K, respectively, and show absorption against the two star-forming Sgr B2(N) hot cores with systematic LSR velocities of +64 (the LMH) and +82 km s⁻¹. These ketenimine data show that the hot core at +82 km s⁻¹ is cooler than the hot core at +64 km s⁻¹. Ketenimine is likely formed directly from its isomer methyl cyanide (CH₃CN) by tautomerization driven by shocks that pervade the star-forming region.

Subject headings: ISM: abundances — ISM: clouds — ISM: individual (Sagittarius B2(N-LMH)) — ISM: molecules — radio lines: ISM

1. INTRODUCTION

Among interstellar molecules, there is a high degree of isomerism, and species with the greatest amount of bonding energy appear to be preferred in space over their less stable isomeric counterparts. For example, of the ~140 known interstellar molecules, about 90 can have stable isomers since all diatomics, a number of hydrogen saturated species, and a few other special species like C₃, CH₂, CH₃, etc., are eliminated from consideration because they have no isomeric counterparts. Currently, among interstellar molecules, there are 13 isomer pairs and three isomer triads, accounting for the statistic that nearly 40% of all interstellar molecules that could have isomeric counterparts do, in fact, have them. Moreover, Remijan et al. (2005) examined observational results toward Sgr B2(N-LMH) for a number of cyanide and isocyanide isomers with respect to bonding energy differences and its effect on whether or not a particular isomer in a set might be formed in sufficient abundance to be detected with current radio telescopes. Furthermore, Lovas et al. (2006) reported studies of the three isomers methylcyanoacetylene (CH₃CCCN), cyanoallene (CH₂CCHCN), and 3-butenitrile (HCCCH₂CN) toward TMC-1 and found that only the isomer with the least bonding energy (shallowest potential well), HCCCH₂CN, was not readily observed. Motivated by these results, the near equivalence in bonding energy of ketenimine (CH₂CNH) and its isomer methyl isocyanide (CH₃NC), a well-studied interstellar species, prompted an interstellar search for ketenimine with the Green Bank Telescope. A successful search was by no means certain because organic imines are relatively rare as interstellar species, with only two previously reported: methyleneimine (CH₂NH) by Godfrey et al. (1973) and 3-imino-1,2-propadienyldiene (CCCNH) by Kawaguchi et al. (1992).

The first spectroscopic identification of ketenimine was ac-

complished by Jacox (1979) with the infrared matrix isolation study of the products from the reaction of excited argon atoms with CH₃CN. This work confirmed an earlier study by Jacox & Milligan (1963) in which ketenimine was tentatively identified as a product of the reaction of the imidyl radical (NH) with acetylene (HCCH) in solid argon. The first study of ketenimine in the gas phase by microwave spectroscopy was reported by Rodler et al. (1984), in which 2-cyanoethanol (HOCH₂CH₂CN) was pyrolyzed at 800°C. The spectrum consisted of *a*-type and *c*-type transitions, and rotational analysis provided the rotational constants $A = 201443.685(75)$ MHz, $B = 9663.138(2)$ MHz, and $C = 9470.127(2)$ MHz. Resolved hyperfine structure was obtained for several transitions, and Stark effect measurements and analysis provided the dipole moment components $\mu_a = 0.434(1)$ D and $\mu_c = 1.371(6)$ D (type A uncertainties with coverage factor $k = 1$; Taylor & Kuyatt 1994). Thus, *c*-type transitions will be more dominant; however, with the *A* rotational constant above 200 GHz, only *P*-branch transitions (or $\Delta J = -1$) will occur in the frequency range of the Green Bank Telescope. A second low-frequency study by Rodler et al. (1986) provided the measurement of the hyperfine structure for the 9_{1,8}–10_{0,10} transition that showed an additional splitting of 131 kHz on each of the hyperfine components. This splitting was interpreted as being due to tunneling of the imino proton through the plane of the ketene portion of the molecule to an equivalent structure, i.e., an inversion motion. This splitting is not observable in the spectral lines reported in § 2. The fitted rotational hyperfine structure reported herein results from an intensity weighted average over the inversion splitting seen by Rodler et al. (1986) and is combined with the data of Rodler et al. (1984) in which no inversion splitting was apparent.

2. OBSERVATIONS AND RESULTS

Spectral line observations of ketenimine were conducted with the NRAO⁴ 100 m Robert C. Byrd Green Bank Telescope

¹ Optical Technology Division, National Institute of Standards and Technology, Gaithersburg, MD 20899.

² NASA Goddard Space Flight Center, Computational and Information Sciences and Technology Office, Code 606, Greenbelt, MD 20771.

³ National Radio Astronomy Observatory, 520 Edgemont Road, Charlottesville, VA 22903-2475.

⁴ The National Radio Astronomy Observatory is a facility of the National Science Foundation, operated under cooperative agreement by Associated Universities, Inc.

TABLE 1
KETENIMINE (CH₂CNH) MOLECULAR LINE PARAMETERS

Transition ($J_{K_a, K_c}^- - J_{K_a, K_c}^+$) (1)	E_l (cm ⁻¹) (2)	S (3)	hfs ($F' - F''$) (4)	Frequency ^a (MHz) (5)	Relative Intensity (6)
9 _{1,8} -10 _{0,10}	35.098	4.425	9-10	4929.916(19)	0.330
			10-11	4930.489(16)	0.365
			8-9	4930.553(17)	0.298
8 _{1,7} -9 _{0,9}	28.717	3.945	8-9	23175.937(24)	0.329
			9-10	23176.504(21)	0.368
			7-8	23176.575(22)	0.294
7 _{1,6} -8 _{0,8}	22.974	3.460	7-8	41523.841(38)	0.328
			8-9	41524.403(35)	0.373
			6-7	41524.484(36)	0.289

^a Ketenimine rest frequencies from present work. Uncertainties in parentheses refer to the least significant digit and are 2 σ values (type A coverage $k = 2$) (Taylor & Kuyatt 1994).

(GBT) on 2005 March 14–22 (Q band), 2005 April 1 (K band), and 2005 September 6–19 (X band). The GBT spectrometer was configured to provide four intermediate-frequency (IF) bandwidths at a time in two polarizations through the use of offset oscillators in the IF. Table 1 lists the molecular parameters of the ketenimine transitions sought: the transition quantum numbers, the lower energy level (E_l), the transition line strength (S), the hyperfine splitting (hfs) quantum numbers, the hfs component rest frequency, and the hfs component relative intensity. Table 2 lists the observational parameters for the search: the ketenimine transition, the telescope beamwidth (θ_B), the telescope beam efficiency (η_B), the spectrometer bandwidth per IF, and the spectrometer channel spacing appear in the first five columns. Antenna temperatures are on the T_A^* scale (Ulich & Haas 1976) with estimated 20% uncertainties. The Sgr B2(N-LMH) J2000 pointing position employed was $\alpha = 17^{\text{h}}47^{\text{m}}19^{\text{s}}.8$, $\delta = -28^{\circ}22'17''$, and an LSR source velocity of +64 km s⁻¹ was assumed. Data were taken in the OFF-ON position-switching mode, with the OFF position 60' east in azimuth with respect to the ON-source position. A single scan consisted of 2 minutes in the OFF-source position followed by 2 minutes in the ON-source position. Automatically updated dynamic pointing and focusing corrections were employed based on real-time temperature measurements of the structure input to a thermal model of the GBT; zero points were adjusted typically every 2 hr or less using the pointing source 1733–130. The two polarization outputs from the spectrometer were averaged in the final data reduction process to improve the signal-to-noise ratio.

Figure 1 shows the three sequential P -branch c -type transitions of ketenimine that were detected in absorption; each spectrum has been processed with a median filter to remove instrumental slopes in the bandpass. For each transition, the integrated line intensity [$W = \int \Delta T_A^*(\nu) d\nu$] and the average source continuum level (T_c), removed by the median filter pro-

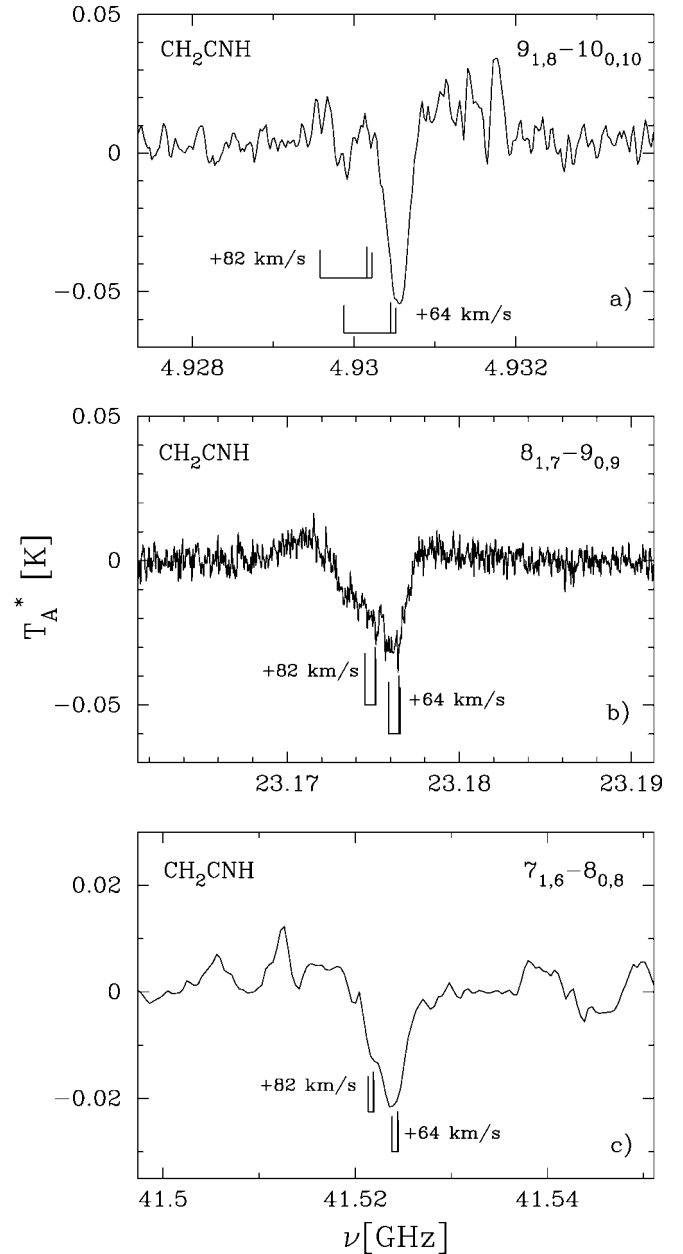


FIG. 1.—Ketenimine spectra toward Sgr B2(N). Transition quantum numbers are shown in each panel. Each abscissa is the rest frequency (see Table 1) at an assumed source velocity of +64 km s⁻¹ with respect to the LSR. In each panel, relative intensity fiducials are shown where hyperfine splitting is expected (see Table 1, col. [6]) for LSR velocities of +64 and +82 km s⁻¹.

TABLE 2
SUMMARY OF OBSERVATIONS TOWARD SGR B2(N-LMH)

Transition ($J_{K_a, K_c}^- - J_{K_a, K_c}^+$) (1)	θ_B (arcsec) (2)	η_B (3)	Bandwidth (MHz) (4)	Resolution (kHz) (5)	W^a (K km s ⁻¹) (6)	T_c (K) (7)	N_T^b (10 ¹⁶ cm ⁻²) (8)
9 _{1,8} -10 _{0,10}	150	0.90	200	24.4	-1.30(20)	38.9	1.26(20)
8 _{1,7} -9 _{0,9}	32	0.75	200	24.4	-1.06(10)	6.0	1.70(16)
7 _{1,6} -8 _{0,8}	18	0.49	800	390.7	-0.59(4)	4.0	1.43(10)

^a Uncertainties in parentheses refer to the least significant digit and are 2 σ values (type A coverage $k = 2$) (Taylor & Kuyatt 1994).

^b Calculations use $\mu_c = 1.371(6)$ D and assume $\theta_s = 5''$ and $T_s = 65$ K (see text); uncertainties reflect the fitting errors on W in col. (6).

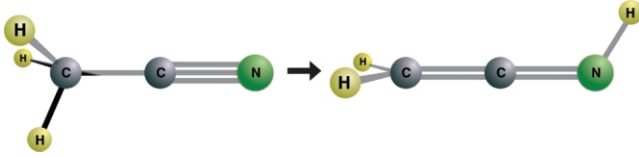


FIG. 2.—Schematic tautomerization reaction diagram showing the molecular structures of methyl cyanide and ketenimine. This isomer conversion reaction may be driven by shocks that pervade the Sgr B2(N) star-forming region (see text).

cessing, are given in Table 2 columns (6) and (7), respectively. Partially resolved hyperfine structure is apparent in Figure 1a at an LSR velocity of $+64 \text{ km s}^{-1}$, which is the systemic velocity of the Large Molecule Heimat (LMH) star-forming core; this $9_{18}-10_{0,10}$ transition at 4.9 GHz has a lower state energy level $\sim 50 \text{ K}$ that is higher in energy than the other two transitions shown in Figure 1. While the $8_{19}-9_{09}$ transition at 23.2 GHz and the $7_{16}-8_{08}$ transition at 41.5 GHz, shown in Figures 1b and 1c, respectively, do not demonstrate evidence of hyperfine splitting, they do display a dominant $+64 \text{ km s}^{-1}$ component and evidence of an $+82 \text{ km s}^{-1}$ shoulder; these LSR velocities are typical of the two star-forming cores within Sgr B2(N). Thus, unlike the lower energy transitions shown in Figures 1b and 1c, the highest energy transition of ketenimine shown in Figure 1a displays a strong $+64 \text{ km s}^{-1}$ component, but nothing appreciable at $+82 \text{ km s}^{-1}$, suggesting that the star-forming core with the $+82 \text{ km s}^{-1}$ systemic velocity is cooler than the $+64 \text{ km s}^{-1}$ star-forming core.

The ketenimine absorption profiles in Figures 1b and 1c and their respective low average source continuum levels (T_c) in Table 2 column (7) can only be reconciled if these transitions are absorbing in compact region(s) in close proximity to the two hot cores. In this instance, beam dilution would boost the observed continuum temperature to ensure that absorption occurs. On the other hand, the ketenimine absorption transition in Figure 1a is the highest energy transition of the three and is observed with the largest telescope beam (see Table 2), so this transition, too, must be absorbing in close proximity to the LMH hot core. Moreover, there is ample observational evidence that the two hot cores with $+64$ and $+82 \text{ km s}^{-1}$ LSR velocities lie superposed along the same line of sight (see Fig. 7 of Mehninger & Menten 1997; and Fig. 2 of Hollis 2006). Thus, to characterize the ketenimine absorption profiles in Figure 1 by a radiative transfer analysis, we make the following key assumptions: (1) All three ketenimine transitions involve same size regions that may not be cospatial, and (2) they can be characterized by a single-state temperature (T_s) in the absorbing region(s). The total column density (N_T) for absorption is

$$N_T = WQ\{\eta_B B(8\pi^3/3h)[T_s - T_c/(\eta_B B)]\mu^2 S \times (e^{-E_l/kT_s} - e^{-E_u/kT_s})\}^{-1}, \quad (1)$$

where the beam dilution factor (B) is given by

$$B = \frac{\theta_s^2}{(\theta_s^2 + \theta_B^2)}. \quad (2)$$

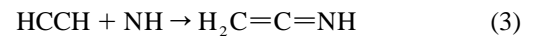
Both equations employ cgs units; parameters that can be obtained directly or derived from the Table 1 and Table 2 parameters include W , θ_B , T_c , E_l , E_u , μ , S , and η_B ; the rotational partition function Q can be approximated as $1.24T_s^{1.5}$. A source size (θ_s)

of $5''$ is assumed and is typical of the size of the LMH (see Fig. 4 of Hollis et al. 2003). Observed integrated line intensities for all three ketenimine transitions were compared to integrated line intensities predicted from equation (1); this method shows that $T_s = 65 \text{ K}$ minimizes the rms difference between the observed and predicted integrated intensities and yields approximately the same total column density (see Table 2 col. [8]). Such a temperature is consistent with a region in proximity to a hot core.

3. DISCUSSION

A new interstellar C₂H₃N isomer triad comprised of CH₃CN and CH₃NC is formed with the detection of interstellar ketenimine. The total column density of equation (1) is a sensitive function of the beam dilution factor of equation (2). For example, using the constraint that minimizes the difference between observed and predicted integrated intensities (see § 2), we find that $T_s \approx 2.07(\theta_s)^2 - 39.14(\theta_s) + 211.5 \text{ K}$ for $4'' \leq \theta_s \leq 10''$. While our assumption that $\theta_s = 5''$ is reasonable, a variation as small as $1''$ has a significant effect on T_s , and therefore the resulting average $\langle N_T \rangle \sim 1.5 \times 10^{16} \text{ cm}^{-2}$ is uncertain by a factor of ~ 2 and can only be refined through interferometric observations to accurately determine the ketenimine source size; similarly, an accurate relative abundance comparison of C₂H₃N isomers also must await complementary interferometric observations. Nevertheless, the ketenimine $\langle N_T \rangle$ determined here is consistent with determinations of total column densities of other molecules observed with interferometers toward Sgr B2(N)—e.g., see Figure 7 of Snyder et al. 2002 for acetic acid (CH₃COOH), formic acid (HCOOH), acetone (CH₃COCH₃), ethyl cyanide (CH₃CH₂CN), and methyl formate (CH₃OCHO). For an H₂ total column density range of $(1-8) \times 10^{25} \text{ cm}^{-2}$ (Lis et al. 1993; Kuan et al. 1996), the ketenimine fractional abundance range is $X = (0.1-3.0) \times 10^{-9}$. Thus, ketenimine is a compact and relatively abundant species in Sgr B2(N).

There are at least three feasible reaction mechanisms suggested by experimental and theoretical studies for the formation of ketenimine in the gas phase or on cold surfaces. From the matrix isolation study by Jacox & Milligan (1963), the following reaction was inferred:



when the reactants were codeposited on a cold argon matrix surface. A subsequent matrix isolation study by Jacox (1979) indicates that energy transfer from argon atoms excited in a microwave discharge can convert methyl cyanide to ketenimine, shown schematically in Figure 2 by tautomerization (i.e., an isomerization pathway in which the migration of a hydrogen atom from the methyl group to the nitrogen atom is accompanied by a rearrangement of bonding electrons). The energetics of this reaction were explored in a theoretical study by Doughty et al. (1994). They found a number of intermediates (including methyl isocyanide) and transition states leading to the formation of ketenimine with methyl isocyanide 38 kJ mol^{-1} ($\sim 2200 \text{ K}$) lower in energy than ketenimine and 95 kJ mol^{-1} ($\sim 5500 \text{ K}$) higher in energy than methyl cyanide. A third route to formation of ketenimine might occur through the ionization of CH₃CN to form CH₃CN⁺ followed by a 1,3 H-shift whose barrier is only 70 kJ mol^{-1} ($\sim 4100 \text{ K}$) on a path to form CH₂CNH⁺. De Petris et al. (2005) calculate that the ketenimine ion is lower in energy than the methyl cyanide ion by 232 kJ mol^{-1} ($\sim 13,500 \text{ K}$) with the small barrier mentioned

above. Subsequent electron capture by the ketenimine ion would yield neutral ketenimine. Further evidence of this isomerization reaction is provided in a mass spectral study of CD_3CN^+ where it was concluded that substantial isomerization occurs on electron impact ionization, resulting in $\text{CD}_2=\text{C}=\text{ND}$ (Mair et al. 2003).

Another laboratory investigation of various cyanide species in ices irradiated by UV photons or bombarded by protons showed imine or isonitrile formation (Hudson & Moore 2004). Proton bombardment of pure CH_3CN ice provided the products ketenimine and CH_3NC in somewhat lower yield. When the CH_3CN ice was irradiated with UV, only CH_3NC was produced. Remijan et al. (2005) cited these results and other studies as supporting their suggestion that isocyanides were not formed primarily in thermal processes.

The tautomerization pathway may be the most applicable to the Sgr B2(N-LMH) region where ketenimine is seen, while the neutral-radical and ionic paths may be more important in other more diffuse and colder interstellar clouds. The Sgr B2(N) region contains widespread shocks (Chengalur & Kanekar 2003) that can provide the energy for both the formation and distribution of large interstellar species. The higher excitation

temperature and compact source required to model the observed transitions suggest that ketenimine is located in a hot core-type region whose high-density gas and dust provide a shield from UV and cosmic rays, which are required to form radicals and ions.

In summary, we have detected ketenimine in absorption toward the Galactic center source Sgr B2(N-LMH) by means of three sequential *c*-type *P*-branch transitions using theGBT. Our analysis of the three absorption lines provides a state temperature of 65 K and a compact source of about $\sim 5''$. Ketenimine is the third isomer detected with the empirical formula $\text{C}_2\text{H}_3\text{N}$ in Sgr B2(N), but it remains to be seen if all three species are cospatial. Laboratory and theoretical studies indicate that ketenimine may be produced by neutral-radical reactions, the ionization of methyl cyanide, or the tautomerization of methyl cyanide.

We thank Cecilia Ceccarelli for reviewing the manuscript, Michael Remijan for programming support and development, and Bill Saxton for graphic art support.

REFERENCES

- Chengalur, J. N., & Kanekar, N. 2003, *A&A*, 403, L43
 de Petris, G., Fornarini, S., Crestoni, M. E., Troiani, A., & Mayer, P. M. 2005, *J. Phys. Chem. A*, 109, 4425
 Doughty, A., Bacskay, G. B., & Mackie, J. C. 1994, *J. Phys. Chem.*, 98, 13546
 Godfrey, P. D., Brown, R. D., Robinson, B. J., & Sinclair, M. W. 1973, *Astrophys. Lett.*, 13, 119
 Hollis, J. M. 2006, in *IAU Symp. 231, Astrochemistry: Recent Successes and Current Challenges*, ed. D. C. Lis, G. A. Blake, & K. A. van der Hucht (New York: Cambridge Univ. Press), 227
 Hollis, J. M., Pedelty, J. A., Boboltz, D. A., Liu, S.-Y., Snyder, L. E., Palmer, P., Lovas, F. J., & Jewell, P. R. 2003, *ApJ*, 596, L235
 Hudson, R. L., & Moore, M. H. 2004, *Icarus*, 172, 466
 Jacox, M. E. 1979, *Chem. Phys.*, 43, 157
 Jacox, M. E., & Milligan, D. E. 1963, *J. Am. Chem. Soc.*, 85, 278
 Kawaguchi, K., et al. 1992, *ApJ*, 396, L49
 Kuan, Y.-J., Mehringer, D. M., & Snyder, L. E. 1996, *ApJ*, 459, 619
 Lis, D. C., Goldsmith, P. F., Carlstrom, J. E., & Scoville, N. Z. 1993, *ApJ*, 402, 238
 Lovas, F. J., Remijan, A. J., Hollis, J. M., Jewell, P. R., & Snyder, L. E. 2006, *ApJ*, 637, L37
 Mair, C., Roithová, J., Fedor, J., Lezius, M., Herman, Z., & Märk, T. D. 2003, *Int. J. Mass Spectrom.*, 223–224, 279
 Mehringer, D. M., & Menten, K. M. 1997, *ApJ*, 474, 346
 Remijan, A. J., Hollis, J. M., Lovas, F. J., Plusquelic, D. F., & Jewell, P. R. 2005, *ApJ*, 632, 333
 Rodler, M. Brown, R. D., Godfrey, P. D., & Kleiböer, B. 1986, *J. Mol. Spectrosc.*, 118, 267
 Rodler, M., Brown, R. D., Godfrey, P. D., & Tack, L. M. 1984, *Chem. Phys. Lett.*, 100, 447
 Snyder, L. E., Lovas, F. J., Mehringer, D. M., Miao, N. Y., Kuan, Y.-J., Hollis, J. M., & Jewell, P. R. 2002, *ApJ*, 578, 245
 Taylor, B. N., & Kuyatt, C. E. 1994, *NIST Tech. Note 1297* (Washington, DC: US GPO)
 Ulich, B. L., & Haas, R. W. 1976, *ApJS*, 30, 247